


## PAPER

[View Article Online](#)  
[View Journal](#) | [View Issue](#)Cite this: *J. Mater. Chem. A*, 2025, **13**, 24868Tailoring dielectric performance *via* dipole density and hydrogen bonding interaction towards high-temperature capacitive energy storage polymers†Feng Zhou, Chong Tian, Lei Huang, Yunfeng Jiang, Fuqi Zhao, Na Yang, Dandan Yuan and Xu-fu Cai \*

In addressing the critical demand for high-performance dielectric materials in advanced energy storage systems at elevated temperatures, this study introduces a molecular engineering strategy integrating copolymerization and polymer blending to optimize dipolar polarization in polyurea-based dielectrics. By systematically modulating the intrinsic molar polarizability through controlled incorporation of small molar volume *m*-phenylenediamine, here we constructed a novel high dipole density co-polyurea with an enhanced dielectric constant. Blending this co-polyurea with polyetherimide disrupted intermolecular hydrogen bonding partially, enhancing free volume and dipole mobility and thus increasing orientational polarizability. Experimental characterization revealed that the 1:1 blend exhibited a remarkably increase in the dielectric constant (7.13), more than twice that of PEI, alongside low dielectric loss (0.0084), high breakdown strength (550 MV m<sup>-1</sup>) and exceptional dielectric thermal stability up to 150 °C. In addition, the polymer blend demonstrated a higher breakdown strength and a lower leakage current density compared to PEI. These properties enabled a discharged energy density of 4.6 J cm<sup>-3</sup> with over 90% charge–discharge efficiency at 150 °C and 400 MV m<sup>-1</sup>, surpassing conventional high-temperature dielectrics. This work establishes a scalable approach to balance dipolar density and dipolar mobility in polar polymers through copolymerization and blending, offering transformative insights for next-generation dielectric capacitors in high-temperature environments.

Received 22nd May 2025  
Accepted 23rd June 2025

DOI: 10.1039/d5ta04136h

[rsc.li/materials-a](https://rsc.li/materials-a)

## 1. Introduction

The recent boom in the development and application of renewable energy sources, such as photovoltaics, wind turbine generators, and electric and hybrid electric vehicles, has generated a significant demand for dielectric capacitors.<sup>1–4</sup> For decades, the state-of-the-art polymer dielectric has been biaxially oriented polypropylene (BOPP) because of its high breakdown strength (>700 MV m<sup>-1</sup>) and low energy loss (tan  $\delta$ , <0.02%) at room temperature.<sup>5,6</sup> However, BOPP has a low dielectric constant ( $\epsilon_r$ ) of 2.25, resulting in a lower energy density and significant volume of the devices.<sup>7,8</sup> In addition, for the BOPP capacitors, the maximum operating temperature is lower than 100 °C, limiting their application under high-power, high-current and elevated-temperature conditions, where the maximum temperature can reach up to 150 °C.<sup>9,10</sup> To meet these demanding requirements, dielectric polymers with a high dielectric constant, low loss and high temperature resistance

are urgently needed for film capacitors in advanced electronic circuits and power systems.<sup>11–14</sup>

Historically, high glass transition temperature ( $T_g$ ) polymers such as polyimide (PI), polyetherimide (PEI), and poly(ether ether ketone) (PEEK) have been recognized as preeminent high-temperature dielectric materials, primarily due to their elevated  $T_g$  values and outstanding thermal stability.<sup>15–17</sup> These properties enable them to maintain structural integrity and dielectric functionality under severe thermal conditions, positioning them as industry standards for high-temperature applications.<sup>11,18</sup> A notable limitation of these established polymers, however, lies in their relatively modest dielectric constants. At 1 kHz and room temperature, for example, PI and PEI exhibit values around 3.1, while PEEK shows a slightly higher but still moderate value of 3.4.<sup>12</sup> Such underwhelming dielectric responses restrict their effectiveness in advanced electrical systems that require strong polarization capabilities alongside thermal resilience. As a result, the development of next-generation high-temperature polymeric dielectrics that can integrate both a high dielectric constant and low dielectric loss remains a significant scientific and engineering challenge.<sup>19–21</sup>

In the quest to further elevate the dielectric properties of polymer dielectrics, a prevalent strategy in materials science entails the incorporation of nanostructured fillers into polymer

College of Polymer Science and Engineering, State Key Laboratory of Polymer Materials Engineering, Sichuan University, Chengdu, 610065, China. E-mail: caixf2008@scu.edu.cn

† Electronic supplementary information (ESI) available. See DOI: <https://doi.org/10.1039/d5ta04136h>

matrices to fabricate nanocomposites, with reported energy densities reaching up to  $5.19 \text{ J cm}^{-3}$  and an efficiency of 80% at  $150^\circ\text{C}$  (PEI/ $\text{Al}_2\text{O}_3@\text{ZrO}_2$ ).<sup>22–24</sup> Yet, the transformative potential of this nanocomposite approach has been overshadowed by two interrelated technical bottlenecks. The first challenge lies in the inadequate homogeneous dispersion of inorganic nanostructured fillers within the polymer matrix, a deficiency that not only induces significant batch-to-batch performance fluctuations but also necessitates reliance on low-dimensional nanofillers (such as nanosheets or nanowires).<sup>25,26</sup> In addition, these fillers, characterized by low synthetic yields and high production costs, pose a substantial barrier to the scalable manufacturing of capacitor films.<sup>27</sup> Compounding this, high-energy-density nanocomposites frequently suffer from subpar charge–discharge efficiencies (usually  $<70\%$ ), a shortfall that can trigger rapid thermal escalation during cyclic operation.<sup>22,28</sup>

Consequently, in the pursuit of enhancing energy storage capabilities in polymer dielectrics, contemporary research has increasingly centered on all-organic polymeric dielectrics, with a notable emphasis on constructing PVDF-based ferroelectric polymers.<sup>29–31</sup> However, empirical investigations reveal a persistent limitation: despite extensive molecular modifications including copolymerization,<sup>32–34</sup> nanocomposite fabrication,<sup>35–37</sup> and crystal phase engineering,<sup>38–40</sup> polarization coupling effects within these ferroelectric matrices remain incompletely mitigated, particularly under intense electric field conditions.<sup>7,16</sup> This unaddressed coupling phenomenon gives rise to pronounced ferroelectric hysteresis loss and escalated conduction losses at high fields. Together, these factors impose a ceiling on energy conversion efficiency and are not suitable for elevated temperatures.

Another viable approach for developing all-organic polymeric dielectrics involves tailoring the polarization of linear polymers.<sup>13,41</sup> Through the incorporation of functional moieties or side chains with specific dipole moments, the net polarization of polymers can be effectively boosted, thereby elevating their dielectric constant.<sup>34,42–45</sup> Among them, urea exhibits a substantial dipole moment of 4.6 Debye, which is significantly higher than that of most polar functional groups, exhibiting exceptional application value in this approach.<sup>46</sup> The pioneering research by Zhang's group first explored aromatic polyurea dielectric films, which demonstrated a combination of advantageous high  $T_g$  and dielectric properties: a relatively high dielectric constant ( $\sim 4.2$ ), an impressive  $E_b$  of  $690 \text{ MV m}^{-1}$ , and negligible leakage current, culminating in a high energy density of  $9 \text{ J cm}^{-3}$  and a charge–discharge efficiency exceeding 95%, with negligible fluctuations in performance observed across a broad temperature spectrum up to  $180^\circ\text{C}$ .<sup>47–51</sup> Building on these foundational findings, subsequent investigations into high-temperature polyurea dielectrics have been conducted; however, the key challenges persist, including balancing dielectric constant with breakdown strength,<sup>52,53</sup> mitigating irreversible long-term thermal degradation,<sup>54–56</sup> addressing complex fabrication and resultant microstructural inhomogeneity.<sup>2,55–57</sup> To overcome these demands, effective design methodologies such as optimizing conjugated molecular architectures, fabricating nanocomposite systems, and implementing blending strategies have emerged.<sup>8,58</sup>

The dielectric constant of polymeric dielectrics can be calculated using the Clausius–Mossotti equation:

$$\epsilon_r = \left(1 + \frac{2P_m}{V_m}\right) / \left(1 - \frac{P_m}{V_m}\right)$$

where  $P_m$  and  $V_m$  denote the molar polarizability and molar volume of atomic groups, respectively. According to the Clausius–Mossotti equation, introducing structural units with high molar polarizability or small molar volume can increase the dielectric constant of dielectrics. In this work, we innovatively propose incorporating *m*-phenylenediamine (MPD) as a third monomer in the polyurea composed of long-chain aromatic diamines. Regulating the ratio of the two diamines allows the control of dipole density, enabling the synthesis of polyurea with enhanced dielectric constants. Meanwhile, polymer blending has been employed to tailor dipole–dipole coupling and intermolecular interactions, modulating chain stacking and spatial distribution to tune free volume and enhance dielectric permittivity. This approach is inherently simple, reliable, and amenable to large-scale industrialization, positioning it as a promising strategy for practical dielectric material development.

Our work endeavors to develop a universally applicable strategy for the design of high-temperature polymer dielectrics utilized in capacitive energy storage, achieved through the integration of molecular structure modulation and polymer blending to optimize dipole-mediated intermolecular hydrogen-bonding interactions. Initially, copolymerization was employed to construct a novel polyurea framework and regulate dipole density. Specifically, MDI and 2,2-bis[4-(4-aminophenoxy)phenyl]propane (BAPOPP) served as primary monomers, with MPD introduced as a comonomer to synthesize the co-polyureas. Subsequent to copolymer synthesis, hydrogen bond networks within the co-polyurea matrix were systematically disrupted by incorporating a non-hydrogen-bonding dipolar glass polymer, PEI, through blending protocols. Experimental results indicated that a 20 mol% MPD content yielded co-polyurea with optimal dielectric characteristics ( $\epsilon_r = 5.1$ ,  $\tan \delta = 0.013$ ), identified as the ideal candidate for blending with PEI. After blending, the 1:1 blend exhibited a significantly enhanced dielectric constant of 7.13, more than twice that of PEI, while retaining low dielectric loss (0.0084) and high breakdown strength ( $550 \text{ MV m}^{-1}$ ). Notably, both the dielectric constant and loss demonstrated excellent thermal stability up to  $150^\circ\text{C}$ . In addition, the polymer blend demonstrated a lower leakage current and a higher breakdown strength compared to PEI, indicating improved insulation performance. The resultant 1:1 blend achieved a discharged energy density of  $4.6 \text{ J cm}^{-3}$  with a charge–discharge efficiency exceeding 90% at  $150^\circ\text{C}$  and  $400 \text{ MV m}^{-1}$ , highlighting its substantial promise for next-generation high-temperature energy storage applications.

## 2. Materials and methods

### 2.1 Materials and synthesis of polyureas

All chemicals used for synthesizing the polyureas: BAPOPP, MDI, MPD, anhydrous *N*-methyl pyrrolidone (NMP) and

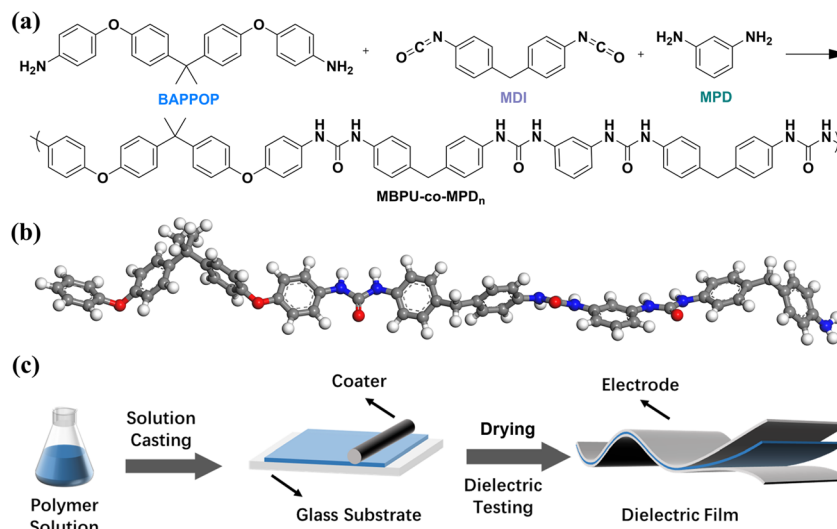


Fig. 1 Synthetic route of MBPU-co-MPD<sub>n</sub> (a), 3D structure of MBPU-co-MPD<sub>n</sub> after geometric configuration optimization (b) and schematic illustration of the dielectric film fabrication (c).

anhydrous methanol were purchased from Adamas-beta. The commercially available PEI (Ultem 1000) was purchased from Sabic. All chemicals and PEI were directly used without other pretreatment or further purification in this work. The novel polyureas (MBPU-co-MPD<sub>n</sub>, *n* represents the molar percentage of MPD in the total diamines) were synthesized from the polycondensation of MDI, BAPOPP and MPD in *N*-methyl-2-pyrrolidone (NMP), as shown in Fig. 1(a). Here, the synthesis of MBPU-co-MPD<sub>10</sub> was exhibited as a representative. BAPOPP (9 mmol), MPD (1 mmol) and NMP were added into the reactor. After complete dissolution, MDI (10.6 mmol) was added, and the reaction mixture was stirred at 60 °C for 12 h under a nitrogen atmosphere. Thereafter, the reaction solution was first diluted 10 times and then dropped into anhydrous methanol to obtain the precipitate. Finally, the precipitated polyurea was washed three times with anhydrous methanol and dried at 80 °C for 12 h under vacuum.

MBPU-co-MPD<sub>n</sub>: <sup>1</sup>H NMR, d-DMSO, δ, ppm, as shown in Fig. S1:† 1.61 (C-CH<sub>3</sub>), 3.80 (Ar-CH<sub>2</sub>-Ar), 6.84–6.96 (Ar-H), 7.10–7.20 (Ar-H), 7.34–7.45 (Ar-H), 8.55–8.60 (HN-C(=O)-NH).

## 2.2 Fabrication of PEI/polyurea blends

All polymer blends were fabricated using the solution casting method as shown in Fig. 1(b).<sup>50</sup> For the standard operating procedure, firstly, the blend solution was obtained by mixing a certain amount of MBPU-co-MPD<sub>n</sub> and PEI in NMP (2 wt%) and stirring at 60 °C for 24 h to completely dissolve the polymers. Secondly, the thin film was prepared by casting the solution onto a clean glass slide and kept in a drying oven at 80 °C for 12 h and 120 °C for 4 h to remove most of the NMP. Thirdly, the as-received film was annealed at 140 °C under vacuum for 12 h to further remove any residual NMP. Finally, the polymer blend film was peeled off from the glass substrate after soaking in deionized water for 10 min, then the films were dried at 70 °C in a vacuum oven for 12 h.

## 2.3 Characterization

**2.3.1 Chemical structure.** Nuclear magnetic resonance (NMR) spectroscopy was carried out on a Bruker AV III HD 400 MHz NMR instrument using deuterium-substituted dimethyl sulfoxide. Fourier transform infrared spectroscopy (FT-IR) was conducted on a Nicolet IS10 Fourier IR spectrometer with a measurement wavenumber of 4000–400 cm<sup>−1</sup>. The intrinsic viscosities ([η]) of the polyureas were determined using an Ubbelohde viscometer based on the following equation:<sup>59</sup>

$$[\eta] = \frac{\sqrt{2(\eta_{sp} - \ln\eta_r)}}{c}$$

where  $\eta_r$  is the relative viscosity,  $\eta_{sp}$  is the specific viscosity and *c* is the concentration of the solution. The concentration of the sample in NMP was 5 g L<sup>−1</sup>, and the measurements were carried out at a constant temperature of 25 ± 0.1 °C. Multiple measurements were performed for each sample, and the average value was calculated from three trials. Gel permeation chromatography (GPC) tests were carried out on an HLC-8320 instrument to evaluate the molecular weights of polyureas. The number-average molecular weight, weight-average molecular weight and polydispersity index were calculated and are summarized in Table S1.†

**2.3.2 Macro and micro-structure.** The digital photos of the dielectric films were taken using a Redmi K40 mobile phone. X-ray diffraction (XRD) patterns were measured using a Rigaku Ultima IV X-ray diffractometer at room temperature. Scans were performed from 5° to 50° at a speed of 5° min<sup>−1</sup>. Scanning electron microscopy (SEM) photographs of the samples were obtained on a Thermo Fisher Scientific Apreo S HiVac scanning electron microscope under high-vacuum conditions at an acceleration voltage of 10 kV.

**2.3.3 Thermal properties.** The *T*<sub>g</sub> of different blend films was tested and evaluated using a TA 850 dynamic thermomechanical analyzer from room temperature to 280 °C, with

a temperature ramp rate of 5 °C min<sup>-1</sup> under a nitrogen atmosphere.

**2.3.4 Dielectric properties.** Before the characterization of dielectric constant and dielectric loss, platinum metal electrodes with a 20 mm diameter were deposited on both surfaces of the polymer films under vacuum conditions using a high-vacuum resistive evaporation coating system. Broadband dielectric spectroscopy was performed using a Novocontrol Concept 50 spectrometer to measure dielectric constants and loss tangents across a frequency spectrum of 10<sup>2</sup> to 10<sup>6</sup> Hz, with temperatures ranging from room temperature to 150 °C. DC breakdown strength evaluations were conducted using a DDJ-50 kV testing apparatus, applying a linear voltage ramp rate of 500 V s<sup>-1</sup> during the measurements.

**2.3.5 Energy storage performance measurements.** The uniaxial electric displacement-electric field (D-E) hysteresis loops served as the basis for deriving discharge energy density (U<sub>e</sub>) and energy storage efficiency (η). In this study, the Premier II system manufactured by Radiant Technologies, Inc. (USA) was utilized to measure the D-E loops of samples at room temperature and 150 °C, respectively. The measurements were conducted at a test frequency of 100 Hz with specimens immersed in silicone oil, where triangular voltage waveforms were applied to obtain D-E loops under varying electric field conditions. Moreover, the leakage current was also characterized under the same conditions.

**2.3.6 Electrostatic potential calculation.** The three-dimensional molecular structures of PEI and MBPU-co-MPD<sub>20</sub> were constructed using Materials Studio software, with electrostatic potential calculations performed based on density functional theory (DFT).<sup>55</sup> In balancing structural accuracy and computational tractability, the DND basis set was selected alongside the BLYP functional for optimizing the geometric configurations of distinct polymer molecules.

### 3. Results and discussion

Polymer blending has been utilized as an economically viable strategy for fabricating high-performance polymer dielectrics.<sup>60</sup> The theoretical framework of blended polymer systems posits that such composites can harmonize the advantageous properties of two distinct polymers. This is achieved through deliberate manipulation of the condensed-phase structure within the polymer matrix and optimization of the functional attributes of organic polymer fillers, ultimately leading to enhanced energy storage capabilities in the resultant materials.<sup>61</sup>

PEI, a widely used high-temperature engineering polymer with a glass transition temperature exceeding 200 °C, exhibits a relatively low dielectric constant. Given the high dipole moment of urea, we synthesized polyurea with enhanced dielectric constants through polymerization of diisocyanates and diamines, subsequently incorporating it into PEI to form polymer blends. From a compatibility perspective, BAPOPP was selected as the diamine monomer due to its structural similarity to PEI. The dielectric constant of polymeric dielectrics can be calculated using the Clausius–Mossotti equation:

$$\epsilon_r = \left(1 + \frac{2P_m}{V_m}\right) / \left(1 - \frac{P_m}{V_m}\right)$$

where  $P_m$  and  $V_m$  denote the molar polarizability and molar volume of atomic groups, respectively. According to the Clausius–Mossotti equation, introducing structural units with high molar polarizability or small molar volume can increase the dielectric constant of dielectrics. Therefore, the longer molecular chain of BAPOPP results in lower dipole density in the resulting polyurea. To address this, we innovatively propose incorporating MPD as a third monomer. Regulating the ratio of the two diamines allows the control of dipole density, enabling the synthesis of polyurea with enhanced dielectric constants. The synthetic route is outlined in Fig. 1(a), with detailed procedures described in the experimental section.

#### 3.1 Chemical structure, dielectric constant and loss of polyureas

The <sup>1</sup>H NMR and FT-IR spectra of polyurea molecules with varying diamine ratios are presented in Fig. 2(a) and (b). In the FT-IR spectra, the absence of N=C=O absorption peaks at 2270 cm<sup>-1</sup> across all samples indicates complete polymerization. The broad peak at 3250–3450 cm<sup>-1</sup> and the absorption near 1550 cm<sup>-1</sup> correspond to the stretching vibrations of the N–H group in polyurea.<sup>19</sup> Besides, the peaks at 2962 and 2930 cm<sup>-1</sup> are assigned to methylene and methyl groups, respectively. The characteristic carbonyl (C=O) stretching vibrations appear at 1652 cm<sup>-1</sup> (hydrogen-bonded C=O) and 1710 cm<sup>-1</sup> (free C=O), confirming polyurea formation.<sup>62,63</sup> The peaks at 1360 cm<sup>-1</sup> reflect the stretching vibrations of CN bonds.<sup>64</sup> Additionally, the <sup>1</sup>H NMR spectra show the disappearance of the chemical shift at 5.4 ppm (attributed to NH<sub>2</sub>) and the emergence of a new peak at 8.55–8.60 ppm (assigned to NH–CO–NH),<sup>58</sup> further confirming the successful synthesis of polyurea.

The molecular weight of a polymer significantly influences its properties. In this study, intrinsic viscosity ([η]) measurements were conducted to compare molecular weight variations across different polyureas. Specifically, the flow time of polymer solutions at identical concentrations was measured using an Ubbelohde viscometer. As shown in Fig. 2(c), increasing the proportion of MPD in the diamine mixture leads to a decrease in intrinsic viscosity, probably due to the steric hindrance effect of BAPOPP, which demonstrates the decrease in degree of polymerization. Notably, when the MPD ratio exceeds 20%, the intrinsic viscosity drops sharply, suggesting a substantial reduction in molecular weight that could pose risks for subsequent performance testing. Moreover, the molecular weights calculated through GPC tests maintain the same trend, and the detailed results are summarized in Table S1.†

The dielectric constant (ε<sub>r</sub>) and loss of the co-polyurea films with varying diamine ratios are presented in Fig. 2(d). Within the test frequency range (10<sup>2</sup> to 10<sup>6</sup> Hz), the dielectric constant decreases gradually with increasing frequency. Notably, the dielectric constants of the films exhibit a progressive enhancement with increasing MPD content, attributable to elevated dipole density arising from the strong dipole moments of urea.



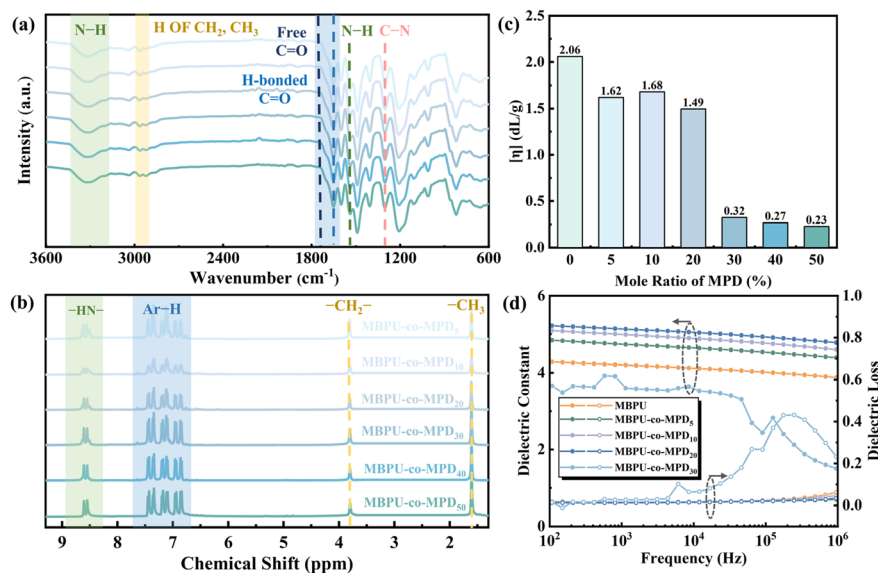


Fig. 2 Chemical structure characterization of MBPU-co-MPD<sub>n</sub>: FT-IR (a), <sup>1</sup>H-NMR (b), intrinsic viscosity (c) and dielectric properties (d).

However, when MPD exceeds 20%, the dielectric constant exhibits obvious frequency-dependent fluctuations, closely correlating with the drop in intrinsic viscosity. This behavior is mainly attributed to increased chain-end effects in lower-molecular-weight polymers, where elevated terminal group concentrations disrupt long-range dipole alignment and introduce structural heterogeneity. In the dielectric loss spectra, minor MPD additions cause negligible changes, whereas contents above 20% trigger significant increases in loss tangent and fluctuations. Given these stability considerations, MBPU-co-MPD<sub>20</sub> was selected for subsequent blending with PEI.

### 3.2 Macro and micro morphology of the PEI/MBPU-co-MPD<sub>20</sub> blends

Polymer blending represents a scalable strategy to enhance dielectric performance by modulating intermolecular interactions, which in turn influences chain packing and

morphological distribution. Prior to investigating PEI/MBPU-co-MPD<sub>20</sub> blends, we characterized the structural and thermal properties of the films to assess miscibility. Macroscopically, all blended films were transparent and homogeneous, with no visual signs of phase separation, indicating a good compatibility between PEI and MBPU-co-MPD<sub>20</sub> in Fig. 3(a). Scanning electron microscopy (SEM) was employed to characterize the microscale morphology of the blends. As depicted in Fig. 3(b), all the blend films exhibited smooth, defect-free surfaces, primarily ascribed to the robust intermolecular hydrogen-bonding interactions established between the urea groups of polyurea and the polar functional groups of PEI.

Moreover, thermodynamic compatibility was further probed *via*  $T_g$  analysis.<sup>65</sup> For miscible polymer systems, a single  $T_g$  intermediate to the  $T_g$  of each component is expected, following the Fox equation:

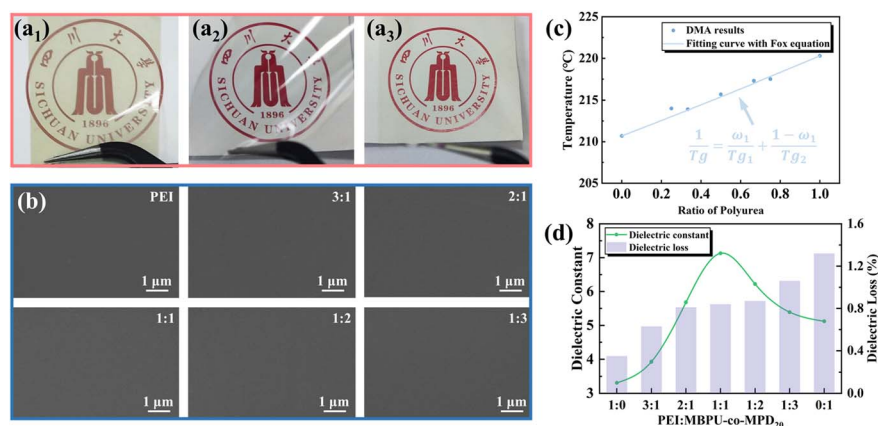


Fig. 3 Digital photographs of PEI (a<sub>1</sub>), MBPU-co-MPD<sub>20</sub> (a<sub>2</sub>), and the 1 : 1 blend (a<sub>3</sub>), SEM images of different ratios of PEI : MBPU-co-MPD<sub>20</sub> (b), DMA results of the loss tangent (c), and dielectric properties of the dielectric films with different blend ratios (d).

$$\frac{1}{T_g} = \frac{\omega_1}{T_{g2}} + \frac{\omega_2}{T_{g1}}$$

where  $T_{g1}$  and  $T_{g2}$  denote the individual  $T_g$  of each polymer, and  $\omega_1$  and  $\omega_2$  are weight fractions. Here, dynamic mechanical analysis (DMA) was applied to investigate the  $T_g$  of polymer blends (Fig. S1†), and the peak of the loss tangent was conventionally applied to determine the  $T_g$  of the polymer. As shown in Fig. 3(c), the resulting thermograms revealed a single, composition-dependent  $T_g$  for all blends, positioned between the higher  $T_g$  of PEI and the lower  $T_g$  of polyurea. Increasing PEI content systematically raised the values of the blends, reflecting improved thermal resistance relative to pure polyurea. Additionally, the excellent agreement between experimental  $T_g$  data and Fox equation predictions underscores molecular-level miscibility, as theoretical calculations closely matched measured values across the composition range in Fig. 3(c).

Overall, the results of DMA and SEM provide robust evidence for the high miscibility of the two polymers. The absence of phase separation in both macroscopic and microscopic analyses confirms that hydrogen bonding effectively promotes molecular-level mixing, validating the suitability of this blending strategy for dielectric property enhancement.

### 3.3 Dielectric properties of PEI/MBPU-co-MPD<sub>20</sub> blends at ambient and elevated temperatures

The dielectric properties of PEI, MBPU-co-MPD<sub>20</sub>, and their blends at different ratios at room temperature and 1 kHz are shown in Fig. 3(d). Notably, all the blends exhibit higher dielectric constants than the original polymers, while the dielectric loss values remain between those of the neat polymers. As the PEI content increases, the dielectric constant increases and reaches a maximum of 7.13 (at 1 kHz) with a low dielectric loss of 0.0084 in the 1 : 1 blend, indicating increases of 115% and 39% over pure PEI and MBPU-co-MPD<sub>20</sub>, respectively. With further increasing the PEI content beyond a 1 : 1 weight ratio, a decrease in dielectric constant is observed. These results suggest that orientational polarization from dipole rotational vibrations in the blend is stronger than in the individual polymers, and reaches a maximum at the 1 : 1 blend ratio. Moreover, the dielectric frequency spectra also show minimal fluctuations across the tested range, demonstrating excellent frequency stability.

For dipolar polymers, the Frohlich model describes the dielectric constant as proportional to both the square of the dipole moment ( $D$ ) and the dipole density ( $N$ ):

$$\frac{(\epsilon_{rs} - \epsilon_{r\infty})(2\epsilon_{rs} + \epsilon_{r\infty})}{\epsilon_{rs}(\epsilon_{r\infty} + 2)^2} = \frac{NgD^2}{9\epsilon_0 k_B T}$$

where  $\epsilon_{rs}$  and  $\epsilon_{r\infty}$  are the low-frequency and optical dielectric constants,  $g$  is the correlation factor,  $\epsilon_0$  is the vacuum permittivity,  $k_B$  is Boltzmann's constant, and  $T$  is the relaxation time. For the polymer blends, though blending may alter intermolecular interactions, affecting chain mobility and dielectric properties. However, as PEI content increases beyond 1 : 1, the decrease in dipole density outweighs the positive effects of

blending, causing the dielectric constant to decline. Here, the 1 : 1 blend was chosen as the optimal dielectric for subsequent characterization.

Prior to characterizing the high-temperature dielectric properties of the polyurea blends, temperature-dependent dielectric spectra were measured for various co-polyureas to evaluate the dielectric thermal stability of the pristine polyurea matrix. As shown in Fig. 4(a)–(d), all co-polyureas exhibit exceptional dielectric thermal stability, with MBPU-co-MPD<sub>20</sub> demonstrating a superior dielectric constant across the temperature range, validating its selection as the optimal co-polyurea for blending with PEI. Owing to the inherent dielectric thermal stability of the pristine polyurea and the high  $T_g$  of the PEI/MBPU-co-MPD<sub>20</sub> blend, all blended polymers retain a stable dielectric constant and loss from 30 to 150 °C. Notably, the 1 : 1 blend exhibits a significantly enhanced dielectric constant compared to both pure PEI and polyurea polymers. Temperature-dependent dielectric spectra of PEI/MBPU-co-MPD<sub>20</sub> blends at different mass ratios (150 °C) are shown in Fig. 4 and S2.†

### 3.4 Analysis of dielectric enhancement mechanisms

To further elucidate the mechanism of dipole motion enhancement through blending, we conducted systematic infrared spectroscopic investigations to quantify the strength of intermolecular interactions in blend films with varying compositions.<sup>56,66</sup> The evolution of hydrogen bonding networks was analyzed through characteristic absorption bands of carbonyl (C=O, hydrogen bond acceptor) and amine (N–H, hydrogen bond donor) groups, where molecular interactions manifest as distinct shifts in peak positions and intensity variations.<sup>67</sup> Fig. 4(g) reveals the characteristic absorption bands corresponding to hydrogen-bonded (1650 cm<sup>−1</sup>) and free carbonyl (1775, 1715 and 1680 cm<sup>−1</sup>) groups.<sup>68</sup> Evidently, the MBPU-co-MPD<sub>20</sub> spectrum exhibits a dominant sharp peak at 1650 cm<sup>−1</sup> with negligible absorption at 1710 cm<sup>−1</sup>, indicating extensive hydrogen bonding formation. Progressive incorporation of PEI induces marked attenuation of the hydrogen-bonded C=O peak intensity. Similar hydrogen bonding effects are observed in the N–H stretching region. The broad absorption band at 3300 cm<sup>−1</sup> for MBPU-co-MPD<sub>20</sub>, characteristic of hydrogen-bonded amine groups, progressively diminishes in intensity with increasing PEI content. These spectroscopic observations confirm that the original N–H/C=O hydrogen-bonding network in polyurea undergoes systematic disruption upon PEI introduction, leading to weakened intermolecular interactions.<sup>69</sup> Moreover, quantitative analysis of hydrogen bond dissociation was performed by calculating the relative fraction of free C=O (Fig. S3†).<sup>70,71</sup> As is evident from the data in Fig. 4(h), the fraction of free C=O demonstrates a nonlinear dependence on blend composition, a sharp increase occurs up to the 1 : 1 blend while remaining practically unchanged at higher PEI concentrations. This transition correlates with reduced dipole moment density in the blends, as PEI possesses lower intrinsic dipole polarity and concentration compared to MBPU-co-MPD<sub>20</sub>. Consequently, the dielectric constant reaches

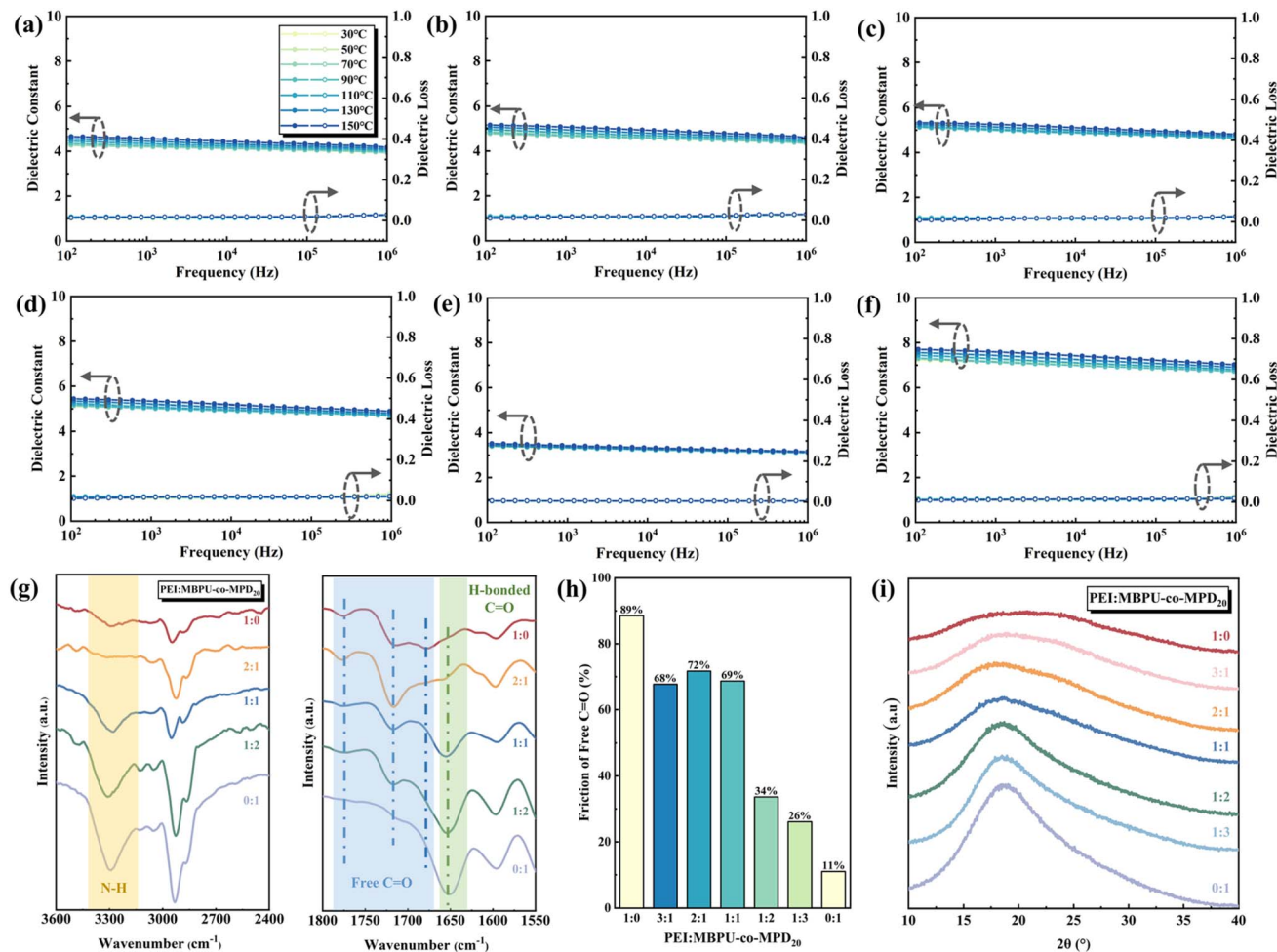


Fig. 4 Dielectric constant and loss of MBPU-co-MPD<sub>0</sub> (a), MBPU-co-MPD<sub>5</sub> (b), MBPU-co-MPD<sub>10</sub> (c), MBPU-co-MPD<sub>20</sub> (d), PEI (e) and the 1 : 1 blend of PEI/MBPU-co-MPD<sub>20</sub> (f) at 150 °C; magnified FT-IR spectra corresponding to the formation of hydrogen bonds (g), friction of free C=O (h) and XRD spectra of PEI/MBPU-co-MPD<sub>20</sub> blends (i).

maximum enhancement at the 1 : 1 blending ratio, reflecting an optimal balance between dipole mobility and density.

Additionally, we employed X-ray diffraction (XRD) to investigate interchain packing and free volume characteristics in polymer blends, providing additional insights into intermolecular hydrogen bonding interactions. As depicted in Fig. 4(i), the XRD pattern of pristine PEI exhibits no distinct diffraction peaks, indicating its amorphous nature. In contrast to PEI, the diffraction peak of MBPU-co-MPD<sub>20</sub> exhibits greater prominence. As the proportion of PEI increases within the blend, a progressive broadening and attenuation of the diffraction peaks are observed. This phenomenon suggests that the incorporation of PEI disrupts intermolecular hydrogen bond networks, thereby reducing the degree of molecular chain alignment and ordered packing induced by such interactions. Concomitantly, the XRD peak positions corresponding to  $2\theta$  angles demonstrate a gradual downshift with higher PEI concentrations, revealing an expansion in average interchain spacing.<sup>52</sup> These XRD observations collectively suggest that PEI incorporation effectively attenuates intermolecular hydrogen

bonding interactions, resulting in less compact chain packing and augmented free volume compared to pristine polyurea.

The experimental evidences demonstrate that PEI weakens the hydrogen bonds in the blend. Generally, the hydrogen bonding network inherently restricts dipole orientation through its strong intermolecular coupling. Therefore, the observed dielectric enhancement in the blends arises primarily from hydrogen bond disruption that directly facilitates dipole realignment. Moreover, the blends also exhibit reduced chain packing density and increased molecular free volume. These synergistic effects collectively enhance dipole mobility within the polymer matrix, thereby elevating the dielectric constant.

### 3.5 Insulating properties

Breakdown strength is a critical parameter for evaluating the insulating properties of dielectric materials. It not only determines the maximum electric field a material can withstand but also indirectly influences its energy storage performance. Dielectric materials typically exhibit probabilistic breakdown

strength distributions due to variations in breakdown pathways under electric fields. The characteristic breakdown strength of the dielectric materials was statistically analyzed using a two-parameter Weibull distribution function:<sup>57</sup>

$$P(E) = 1 - e^{-\left(\frac{E}{E_b}\right)^\beta}$$

where  $P(E)$  represents the cumulative breakdown probability,  $E$  is the experimentally measured breakdown strength,  $E_b$  denotes the Weibull characteristic breakdown strength at 63.2% cumulative probability, and  $\beta$  is the shape factor related to breakdown dispersion. Fig. 5(a) presents the Weibull characteristic breakdown strengths of these polymer dielectric films at ambient temperature, with corresponding results shown in Fig. 5(b). As polyurea content increases in the blend films, breakdown strength increases from 446 MV m<sup>-1</sup> for pure PEI to 624 MV m<sup>-1</sup> for MBPU-co-MPD<sub>20</sub>. Notably, MBPU-co-MPD<sub>20</sub> exhibits a dielectric breakdown strength  $\sim 1.3$ -fold higher than PEI, primarily attributed to strong hydrogen bonding between polyurea chains that induces compact molecular packing. This dense structure, confirmed by XRD measurements, effectively mitigates structural defects, promotes uniform electric field distribution, and enhances breakdown resistance. Even the 1 : 1 blend, though showing reduced breakdown strength relative to

MBPU-co-MPD<sub>20</sub>, exceeds 550 MV m<sup>-1</sup>, demonstrating excellent insulating properties. Moreover, the high Weibull shape factor  $\beta$  further validates the reliability of the breakdown measurements.

### 3.6 Energy storage performance

The polarization behaviors of PEI, MBPU-co-MPD<sub>20</sub> and the 1 : 1 blend at room temperature and 150 °C were investigated using unipolar D-E loops (Fig. S4†). At room temperature, all dipolar polymers exhibit slim D-E loops, indicating that the incorporation of polyurea does not induce ferroelectric domains. When heated to 150 °C, the loops gradually broaden with increasing electric field, suggesting enhanced dipole alignment and higher dielectric loss under high-field conditions. The energy storage performance of the dielectrics was evaluated based on D-E loops. By integrating the hysteresis loop, the discharged energy storage density of dielectrics can be obtained. Additionally, the charge-discharge efficiency, defined as the ratio of discharged energy density to charged energy density, is also a key parameter for dielectric materials. Low efficiency implies that most energy stored during charging is dissipated as Joule heat rather than electrical energy during discharge, leading to internal over-heating and a sharp decline in breakdown strength. Thus, high charge-discharge efficiency is crucial for both operational

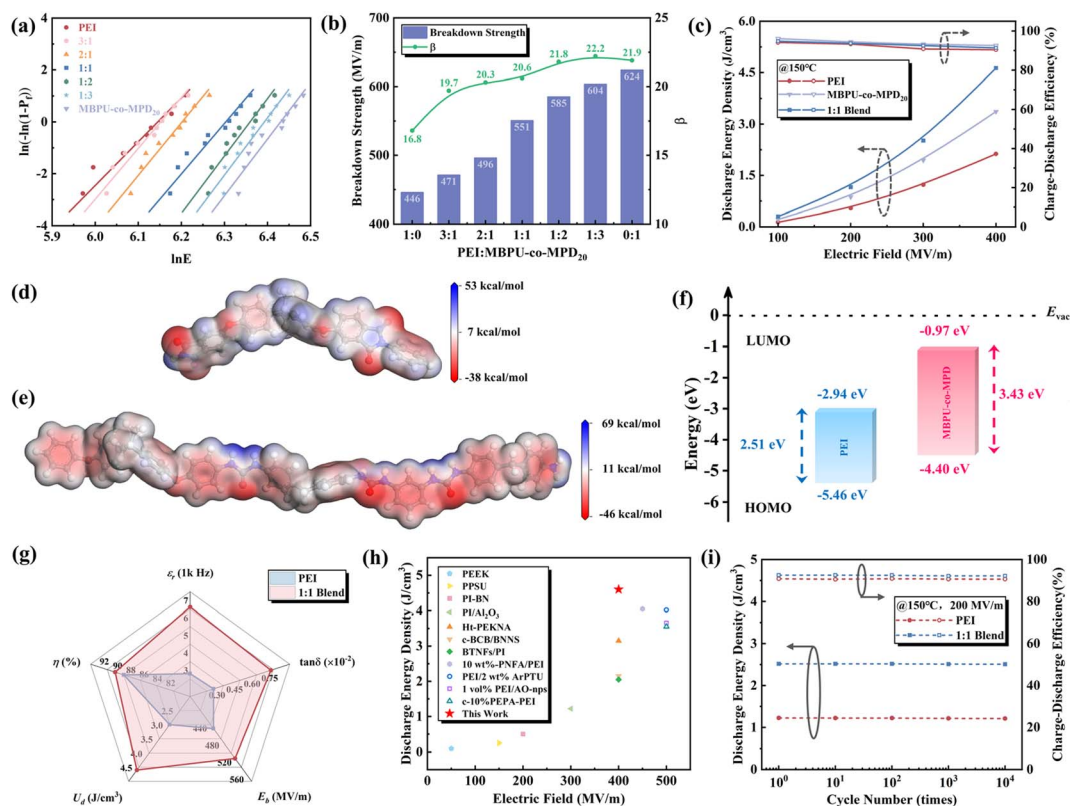


**Fig. 5** Weibull breakdown characteristics (a). Variation of breakdown strength versus the mass ratio of PEI/MBPU-co-MPD<sub>20</sub> blends (b). Energy storage properties of PEI, MBPU-co-MPD<sub>20</sub>, and the 1 : 1 blend at 150 °C (c). Surface electrostatic potential distribution of PEI (d) and MBPU-co-MPD<sub>20</sub> (e). HOMO and LUMO energy levels (f) of PEI and MBPU-co-MPD<sub>20</sub>. Radar chart of capacitive performance of PEI and the 1 : 1 blend at 150 °C (g). Reported discharged energy density of the advanced polymer dielectrics at above 90% charge-discharge efficiency at 150 °C (h). Cycling stability of energy storage performance over 10<sup>4</sup> cycles at 150 °C (i).



effectiveness and longevity. Fig. S5† and 5(c) exhibit the discharged energy densities and efficiencies of dipolar polymers at room temperature and 150 °C. While energy density increases significantly with electric field, charge-discharge efficiency gradually decreases due to conductive and polarization loss. Benefiting from the high dielectric constant and breakdown strength, the 1 : 11 : 1 blended dielectric achieves a discharged energy density of 5.1 J cm<sup>-3</sup> with over 95% efficiency at 25 °C and 400 MV m<sup>-1</sup>. Remarkably, the 1 : 1 blend retains excellent high-temperature energy storage performance, delivering a discharged energy density of 4.6 J cm<sup>-3</sup> with over 90% efficiency at 150 °C and 400 MV m<sup>-1</sup>, almost 117% higher than that of pure PEI.

In polymer dielectrics, elevated temperatures promote electron-hopping conduction and charge carrier migration, exacerbating conductive loss and reducing the energy storage efficiency.<sup>72</sup> As illustrated in Fig. S5,† the leakage current density of PEI increases rapidly with the rise in electric field strength, whereas polyurea exhibits a lower leakage current density that grows gradually as the electric field increases. On the one hand, the strong intermolecular hydrogen bond interactions in polyurea enable more compact packing of polymer chains, which restricts the movement of polymer segments and effectively suppresses the expansion of charge migration pathways at high temperatures. On the other hand, results from molecular electrostatic potential simulations indicate that polyurea has a higher maximum positive electrostatic potential than PEI (Fig. 5(d), (e) and S5†). This characteristic allows polyurea to act as trap sites for capturing charges in an electric field, thereby further reducing the leakage current. Besides, the calculated HOMO and LUMO energy levels are shown in Fig. 5(f). The wider bandgap of the polyurea can further suppress thermally or electrically induced carrier generation, minimizing leakage currents. In the 1 : 1 blend, although the leakage current value increases slightly, it still remains below 10<sup>-7</sup> Amp cm<sup>-2</sup>, demonstrating excellent insulating properties.

The overall capacitive properties of PEI and the 1 : 1 blend at 150 °C are concluded in the radar charts in Fig. 5(g). In addition, Fig. 5(h) illustrates the discharged energy density of state-of-the-art polymer dielectrics reported at above 90% charge-discharge efficiency at 150 °C.<sup>22,26,56,57,72–80</sup> Among them, the PEI/MBPU-co-MPD<sub>20</sub> blend in our work exhibited the highest discharged energy density under 400 MV m<sup>-1</sup>, indicating the potential of the PEI/MBPU-co-MPD<sub>20</sub> blended polymer as a promising candidate for high-temperature energy storage applications.

The cycling stability of PEI and the 1 : 1 blended polymer dielectric film was investigated at 150 °C. As depicted in Fig. 5(g), all dielectric films maintain favorable stability over 10 000 cycles. Positioning it as a promising candidate for high-temperature electronic applications.

## 4. Conclusions

The synergistic integration of co-polymer design and blending methods demonstrated herein provides a robust strategy for engineering high-temperature polymer dielectrics with

optimized energy storage capability. By strategically tailoring the intrinsic molar polarizability through MPD incorporation and disrupting hydrogen bonds *via* PEI blending, we overcame the inherent trade-off between dipolar density and dipole mobility in polar polymers, achieving a notable enhancement in dielectric constant without compromising dielectric loss and high-temperature dielectric properties. In addition, the polymer blend demonstrated a lower leakage current and a higher breakdown strength compared to PEI. The resultant copolyurea/PEI blend represents a discharged energy density of 4.6 J cm<sup>-3</sup> with a charge-discharge efficiency exceeding 90% at 150 °C and 400 MV m<sup>-1</sup>, almost 117% higher than that of pure PEI, for meeting the stringent requirements of next-generation electrical systems. Our work exhibits a paradigm shift from traditional filler-based composites, showcasing the power of all-organic molecular engineering to address long-standing limitations in dielectric materials.

## Data availability

All data supporting this study are included in the article and its ESI.†

## Conflicts of interest

There are no conflicts to declare.

## Acknowledgements

This research was supported by the Key Laboratory of Fine Chemical Application Technology of Luzhou (No. HYJH-2103-A).

## References

- 1 C. Liu, F. Li, L. P. Ma and H. M. Cheng, Advanced materials for energy storage, *Adv. Mater.*, 2010, **22**(8), E28.
- 2 X. Wu, X. Chen, Q. M. Zhang and D. Q. Tan, Advanced dielectric polymers for energy storage, *Energy Storage Mater.*, 2022, **44**, 29.
- 3 H. Zhang, T. Wei, Q. Zhang, W. Ma, P. Fan, D. Salamon, S.-T. Zhang, B. Nan, H. Tan and Z.-G. Ye, A review on the development of lead-free ferroelectric energy-storage ceramics and multilayer capacitors, *J. Mater. Chem. C*, 2020, **8**(47), 16648.
- 4 M. Yang, M. Guo, E. Xu, W. Ren, D. Wang, S. Li, S. Zhang, C. W. Nan and Y. Shen, Polymer nanocomposite dielectrics for capacitive energy storage, *Nat. Nanotechnol.*, 2024, **19**(5), 588.
- 5 C.-Q. Li, J.-W. Zha, H.-Q. Long, S.-J. Wang, D.-L. Zhang and Z.-M. Dang, Mechanical and dielectric properties of graphene incorporated polypropylene nanocomposites using polypropylene-graft-maleic anhydride as a compatibilizer, *Compos. Sci. Technol.*, 2017, **153**, 111.
- 6 Z. Xie, R. Xue, Z. Dou, L. Xiao, Y. Li, Q. Zhang and Q. Fu, Largely enhanced dielectric and thermal conductive properties of polypropylene composites by adding mixture

- of exfoliated boron nitride and liquid metal, *Composites, Part A*, 2022, **161**, 107081.
- 7 J. Chen, Z. Pei, B. Chai, P. Jiang, L. Ma, L. Zhu and X. Huang, Engineering the dielectric constants of polymers: from molecular to mesoscopic scales, *Adv. Mater.*, 2024, **36**(52), e2308670.
  - 8 H. Luo, F. Wang, R. Guo, D. Zhang, G. He, S. Chen and Q. Wang, Progress on polymer dielectrics for electrostatic capacitors application, *Adv. Sci.*, 2022, **9**(29), e2202438.
  - 9 N. Yang, F. Zeng, D. Yuan and X. Cai, Hydrogen-bond-free piperazine polyamides with ultralow dielectric loss, *Ind. Eng. Chem. Res.*, 2024, **63**(26), 11436.
  - 10 M. D. Zahidul Islam, Y. Fu, H. Deb, M. D. Khalid Hasan, Y. Dong and S. Shi, Polymer-based low dielectric constant and loss materials for high-speed communication network: dielectric constants and challenges, *Eur. Polym. J.*, 2023, **200**, 112543.
  - 11 R. Bian, P. Liao, C. Zhou, B. Jiang, Y. Deng, Y. Zhang, Y. Shang and H. Zhang, Enhancing high-temperature capacitive performance of polyetherimide composites through hydrogen bonding, *J. Power Sources*, 2025, **640**, 236817.
  - 12 M. Yang, W. Ren, Z. Jin, E. Xu and Y. Shen, Enhanced high-temperature energy storage performances in polymer dielectrics by synergistically optimizing band-gap and polarization of dipolar glass, *Nat. Commun.*, 2024, **15**(1), 8647.
  - 13 J. Wei and L. Zhu, Intrinsic polymer dielectrics for high energy density and low loss electric energy storage, *Prog. Polym. Sci.*, 2020, **106**, 101254.
  - 14 L. Zhu, Exploring strategies for high dielectric constant and low loss polymer dielectrics, *J. Phys. Chem. Lett.*, 2014, **5**(21), 3677.
  - 15 Y. Qiao, X. Yin, T. Zhu, H. Li and C. Tang, Dielectric polymers with novel chemistry, compositions and architectures, *Prog. Polym. Sci.*, 2018, **80**, 153.
  - 16 R. Wang, Y. Zhu, J. Fu, M. Yang, Z. Ran, J. Li, M. Li, J. Hu, J. He and Q. Li, Designing tailored combinations of structural units in polymer dielectrics for high-temperature capacitive energy storage, *Nat. Commun.*, 2023, **14**(1), 2406.
  - 17 W. Huang, T. Ju, R. Li, Y. Duan, Y. Duan, J. Wei and L. Zhu, High- $\kappa$  and high-temperature dipolar glass polymers based on sulfonylated and cyanolated poly(arylene ether)s for capacitive energy storage, *Adv. Electron. Mater.*, 2022, **9**(1).
  - 18 S. Anwar, M. Hassanpour Amiri, S. Jiang, M. M. Abolhasani, P. R. F. Rocha and K. Asadi, Piezoelectric nylon-11 fibers for electronic textiles, energy harvesting and sensing, *Adv. Funct. Mater.*, 2020, **31**(4), 2004326.
  - 19 D. Yuan, Y. Xu, L. Huang, J. Ma, Q. Peng, Y. Ren, W. Li and X. Cai, Novel prominent nylon-1 with excellent dielectric properties and a high Curie point, *J. Mater. Chem. C*, 2019, **7**(6), 1641.
  - 20 D. Yuan, Y. Xu, F. Zhou and X. Cai, Synthesis and characterization of multifunctional polyamide 1 using CO<sub>2</sub> and urea via environment-friendly method, *J. Polym. Sci., Part A: Polym. Chem.*, 2018, **56**(8), 853.
  - 21 J. Wei, T. Ju, W. Huang, J. Song, N. Yan, F. Wang, A. Shen, Z. Li and L. Zhu, High dielectric constant dipolar glass polymer based on sulfonylated poly(ether ether ketone), *Polymer*, 2019, **178**, 121688.
  - 22 Q. Li, L. Chen, M. R. Gadinski, S. Zhang, G. Zhang, U. Li, E. Iagodkine, A. Haque, L. Q. Chen, N. Jackson, *et al.*, Flexible high-temperature dielectric materials from polymer nanocomposites, *Nature*, 2015, **523**(7562), 576.
  - 23 L. Ren, H. Li, Z. Xie, D. Ai, Y. Zhou, Y. Liu, S. Zhang, L. Yang, X. Zhao, Z. Peng, *et al.*, High-temperature high-energy-density dielectric polymer nanocomposites utilizing inorganic core-shell nanostructured nanofillers, *Adv. Energy Mater.*, 2021, **11**(28), 2101297.
  - 24 Y. Zhu, Y. Zhu, X. Huang, J. Chen, Q. Li, J. He and P. Jiang, High energy density polymer dielectrics interlayered by assembled boron nitride nanosheets, *Adv. Energy Mater.*, 2019, **9**(36), 1901826.
  - 25 J. Dong, R. Hu, X. Xu, J. Chen, Y. Niu, F. Wang, J. Hao, K. Wu, Q. Wang and H. Wang, A facile in situ surface-functionalization approach to scalable laminated high-temperature polymer dielectrics with ultrahigh capacitive performance, *Adv. Funct. Mater.*, 2021, **31**(32), 2102644.
  - 26 M. Fan, P. Hu, Z. Dan, J. Jiang, B. Sun and Y. Shen, Significantly increased energy density and discharge efficiency at high temperature in polyetherimide nanocomposites by a small amount of Al<sub>2</sub>O<sub>3</sub> nanoparticles, *J. Mater. Chem. A*, 2020, **8**(46), 24536.
  - 27 W. Ren, J. Pan, Z. Dan, T. Zhang, J. Jiang, M. Fan, P. Hu, M. Li, Y. Lin, C.-W. Nan, *et al.*, High-temperature electrical energy storage performances of dipolar glass polymer nanocomposites filled with trace ultrafine nanoparticles, *Chem. Eng. J.*, 2021, **420**, 127614.
  - 28 Y. Zhou, C. Yuan, S. Wang, Y. Zhu, S. Cheng, X. Yang, Y. Yang, J. Hu, J. He and Q. Li, Interface-modulated nanocomposites based on polypropylene for high-temperature energy storage, *Energy Storage Mater.*, 2020, **28**, 255.
  - 29 B. Li, M. Yuan, S. Zhang, R. Rajagopalan and M. T. Lanagan, Abnormal high voltage resistivity of polyvinylidene fluoride and implications for applications in high energy density film capacitors, *Appl. Phys. Lett.*, 2018, **113**(19), 193903.
  - 30 L. Yang, X. Li, E. Allahyarov, P. L. Taylor, Q. M. Zhang and L. Zhu, Novel polymer ferroelectric behavior via crystal isomorphism and the nanoconfinement effect, *Polymer*, 2013, **54**(7), 1709.
  - 31 M. Yuan, B. Li, S. Zhang, R. Rajagopalan and M. T. Lanagan, High-field dielectric properties of oriented poly(vinylidene fluoride-co-hexafluoropropylene): structure-dielectric property relationship and implications for energy storage applications, *ACS Appl. Polym. Mater.*, 2020, **2**(3), 1356.
  - 32 N. Meng, X. Ren, X. Zhu, J. Wu, B. Yang, F. Gao, H. Zhang, Y. Liao, E. Bilotti, M. J. Reece, *et al.*, Multiscale understanding of electric polarization in poly(vinylidene fluoride)-based ferroelectric polymers, *J. Mater. Chem. C*, 2020, **8**(46), 16436.
  - 33 K. Yin, Z. Zhou, D. E. Schuele, M. Wolak, L. Zhu and E. Baer, Effects of interphase modification and biaxial orientation on

- dielectric properties of poly(ethylene terephthalate)/poly(vinylidene fluoride-co-hexafluoropropylene) multilayer films, *ACS Appl. Mater. Interfaces*, 2016, **8**(21), 13555.
- 34 Y. Li, T. Soulestin, V. Ladmira, B. Ameduri, T. Lannuzel, F. Domingues Dos Santos, Z.-M. Li, G.-J. Zhong and L. Zhu, Stretching-induced relaxor ferroelectric behavior in a poly(vinylidene fluoride-co-trifluoroethylene-co-hexafluoropropylene) random terpolymer, *Macromolecules*, 2017, **50**(19), 7646.
  - 35 D. Prateek, V. K. Thakur and R. K. Gupta, Recent progress on ferroelectric polymer-based nanocomposites for high energy density capacitors: synthesis, dielectric properties, and future aspects, *Chem. Rev.*, 2016, **116**(7), 4260.
  - 36 J. Li, Z. Jing, Y. Yang, F. Zha, L. Yan and Z. Lei, Reversible low adhesive to high adhesive superhydrophobicity transition on ZnO nanoparticle surfaces, *Appl. Surf. Sci.*, 2014, **289**, 1.
  - 37 Y. Xie, Y. Yu, Y. Feng, W. Jiang and Z. Zhang, Fabrication of stretchable nanocomposites with high energy density and low loss from cross-linked PVDF filled with poly(dopamine) encapsulated BaTiO<sub>3</sub>, *ACS Appl. Mater. Interfaces*, 2017, **9**(3), 2995.
  - 38 X. Zhang, Y. Zhao, Y. Wu and Z. Zhang, Poly(tetrafluoroethylene-hexafluoropropylene) films with high energy density and low loss for high-temperature pulse capacitors, *Polymer*, 2017, **114**, 311.
  - 39 Y. Zhang, G. Zhao, S. M. Chapal Hossain and X. He, Modeling and experimental studies of enhanced cooling by medical gauze for cell cryopreservation by vitrification, *Int. J. Heat Mass Transf.*, 2017, **114**, 1.
  - 40 P. Martins, A. C. Lopes and S. Lanceros-Mendez, Electroactive phases of poly(vinylidene fluoride): determination, processing and applications, *Prog. Polym. Sci.*, 2014, **39**(4), 683.
  - 41 Y. Thakur, M. Lin, S. Wu, Z. Cheng, D. Y. Jeong and Q. M. Zhang, Tailoring the dipole properties in dielectric polymers to realize high energy density with high breakdown strength and low dielectric loss, *J. Appl. Phys.*, 2015, **117**(11), 114104.
  - 42 M. Feng, Y. Feng, T. Zhang, J. Li, Q. Chen, Q. Chi and Q. Lei, Recent advances in multilayer-structure dielectrics for energy storage application, *Adv. Sci.*, 2021, **8**(23), e2102221.
  - 43 H. Pan, A. Kursumovic, Y. H. Lin, C. W. Nan and J. L. MacManus-Driscoll, Dielectric films for high performance capacitive energy storage: multiscale engineering, *Nanoscale*, 2020, **12**(38), 19582.
  - 44 Z. Zhang, D. H. Wang, M. H. Litt, L. S. Tan and L. Zhu, High-temperature and high-energy-density dipolar glass polymers based on sulfonylated poly(2,6-dimethyl-1,4-phenylene oxide), *Angew. Chem., Int. Ed. Engl.*, 2018, **57**(6), 1528.
  - 45 Y.-F. Zhu, Z. Zhang, M. H. Litt and L. Zhu, High dielectric constant sulfonyl-containing dipolar glass polymers with enhanced orientational polarization, *Macromolecules*, 2018, **51**(16), 6257.
  - 46 A. Banihashemi, H. Hazarkhani and A. Abdolmaleki, Efficient and rapid synthesis of polyureas and polythioureas from the reaction of urea and thiourea with diamines under microwave irradiation, *J. Polym. Sci., Part A: Polym. Chem.*, 2004, **42**(9), 2106.
  - 47 Q. Burlingame, S. Wu, M. Lin and Q. M. Zhang, Conduction mechanisms and structure-property relationships in high energy density aromatic polythiourea dielectric films, *Adv. Energy Mater.*, 2013, **3**(8), 1051.
  - 48 Z. Cheng, M. Lin, S. Wu, Y. Thakur, Y. Zhou, D.-Y. Jeong, Q. Shen and Q. M. Zhang, Aromatic poly(arylene ether urea) with high dipole moment for high thermal stability and high energy density capacitors, *Appl. Phys. Lett.*, 2015, **106**(20), 202902.
  - 49 Y. Wang, X. Zhou, M. Lin and Q. M. Zhang, High-energy density in aromatic polyurea thin films, *Appl. Phys. Lett.*, 2009, **94**(20), 202905.
  - 50 S. Wu, W. Li, M. Lin, Q. Burlingame, Q. Chen, A. Payzant, K. Xiao and Q. M. Zhang, Aromatic polythiourea dielectrics with ultrahigh breakdown field strength, low dielectric loss, and high electric energy density, *Adv. Mater.*, 2013, **25**(12), 1734.
  - 51 S. Wu, M. Lin, Q. Burlingame and Q. M. Zhang, Meta-aromatic polyurea with high dipole moment and dipole density for energy storage capacitors, *Appl. Phys. Lett.*, 2014, **104**(7), 072903.
  - 52 Q. Zhang, X. Chen, B. Zhang, T. Zhang, W. Lu, Z. Chen, Z. Liu, S. H. Kim, B. Donovan, R. J. Warzoha, *et al.*, High-temperature polymers with record-high breakdown strength enabled by rationally designed chain-packing behavior in blends, *Matter*, 2021, **4**(7), 2448.
  - 53 V. Jurečić, N. Novak, L. Fulanović and V. Bobnar, Space charge contributions to the dielectric response and breakdown strength of high-temperature poly(ether imide)/polyimide blends, *Macromolecules*, 2023, **56**(3), 1097.
  - 54 Y. Thakur, R. Dong, M. Lin, S. Wu, Z. Cheng, Y. Hou, J. Bernholc and Q. M. Zhang, Optimizing nanostructure to achieve high dielectric response with low loss in strongly dipolar polymers, *Nano Energy*, 2015, **16**, 227.
  - 55 J. Yan, B. Liu, J. Wang, J. Zeng, B. Li, X. Zhang, S. Zhang and C.-W. Nan, Optimized molecular interactions significantly enhance capacitive energy storage in polymer blends at 150 °C, *Energy Storage Mater.*, 2025, **74**, 103919.
  - 56 C. Zhou, W. Xu, Y. Zhang, C. Yu, X. Liu, Z. Jiang, C. Zhang, Y. Shang and H. Zhang, Hydrogen bonding of aramid boosts high-temperature capacitive properties of polyetherimide blends, *ACS Appl. Mater. Interfaces*, 2023, **15**(6), 8471.
  - 57 Y. Zhang, Y. Guo, Y. Liu, Z. Shi, W. Liu, J. Su, G. Chen and D. Zhou, All-organic ArPTU/PEI composite dielectric films with high-temperature resistance and high energy-storage density, *J. Mater. Chem. C*, 2024, **12**(12), 4426.
  - 58 Z. Zhao, Y. Feng, L. Yang, S. Zhang, X. Liu, Y. Zhang, M. Li and S. Li, Optimizing the conjugated structure of aromatic polyurea for high-temperature capacitive energy storage, *Appl. Phys. Lett.*, 2023, **123**(23), 232901.
  - 59 D. Yuan, J. Bao, Y. Ren, W. Li, L. Huang and X. Cai, Synthesis of nylon 1 in supercritical carbon dioxide and its crystallization behavior effect on nylon 11, *CrystEngComm*, 2018, **20**(32), 4676.

- 60 W. F. Yong and T. S. Chung, Mechanically strong and flexible hydrolyzed polymers of intrinsic microporosity (PIM-1) membranes, *J. Polym. Sci., Part B: Polym. Phys.*, 2017, **55**(4), 344.
- 61 Y. Zhou, Y. Zhao, F. Chen, Y. Chen, Q. Liu, X. He, X. Mao, Y. Yang and J. Xu, Poly(vinylidene fluoride-co-chlorotrifluoroethylene) and polyurea composite with enhanced energy storage properties, *J. Mater. Sci.: Mater. Electron.*, 2019, **30**(10), 9259.
- 62 C. Tian, F. Zhao, N. Yang, Y. Jiang, L. Huang, F. Zhou, D. Yuan and X. Cai, Durable, super-resilient, and ultra-strong polyurethane elastomers *via* a dense hydrogen bond cross-linking strategy, *Macromolecules*, 2025, **58**(6), 2905.
- 63 J.-H. Choi and M. Cho, Calculations of intermode coupling constants and simulations of amide I, II, and III vibrational spectra of dipeptides, *Chem. Phys.*, 2009, **361**(3), 168.
- 64 T. J. Zimudzi, K. E. Feldman, J. F. Sturnfield, A. Roy, M. A. Hickner and C. M. Stafford, Quantifying carboxylic acid concentration in model polyamide desalination membranes *via* Fourier transform infrared spectroscopy, *Macromolecules*, 2018, **51**(17), 6623–6629.
- 65 Y. Thakur, B. Zhang, R. Dong, W. Lu, C. Iacob, J. Runt, J. Bernholc and Q. M. Zhang, Generating high dielectric constant blends from lower dielectric constant dipolar polymers using nanostructure engineering, *Nano Energy*, 2017, **32**, 73.
- 66 Q. Zhang, X. Chen, T. Zhang and Q. M. Zhang, Giant permittivity materials with low dielectric loss over a broad temperature range enabled by weakening intermolecular hydrogen bonds, *Nano Energy*, 2019, **64**, 103916.
- 67 S. Liu, M. Tian, B. Yan, Y. Yao, L. Zhang, T. Nishi and N. Ning, High performance dielectric elastomers by partially reduced graphene oxide and disruption of hydrogen bonding of polyurethanes, *Polymer*, 2015, **56**, 375.
- 68 J. Verjans and R. Hoogenboom, Supramolecular polymer materials based on ureidopyrimidinone quadruple hydrogen bonding units, *Prog. Polym. Sci.*, 2023, **142**, 101689.
- 69 N. Lou, Y. Wang, H. Li, A. P. Sokolov and H. Xiong, Glassy dynamics of hydrogen-bonded heteroditopic molecules, *Polymer*, 2012, **53**(20), 4455.
- 70 H. Ying, Y. Zhang and J. Cheng, Dynamic urea bond for the design of reversible and self-healing polymers, *Nat. Commun.*, 2014, **5**, 3218.
- 71 M. Tian, B. Yan, Y. Yao, L. Zhang, T. Nishi and N. Ning, Largely improved actuation strain at low electric field of dielectric elastomer by combining disrupting hydrogen bonds with ionic conductivity, *J. Mater. Chem. C*, 2014, **2**(39), 8388.
- 72 H. Li, Y. Zhou, Y. Liu, L. Li, Y. Liu and Q. Wang, Dielectric polymers for high-temperature capacitive energy storage, *Chem. Soc. Rev.*, 2021, **50**(11), 6369.
- 73 D. Ai, H. Li, Y. Zhou, L. Ren, Z. Han, B. Yao, W. Zhou, L. Zhao, J. Xu and Q. Wang, Tuning Nanofillers in *in situ* prepared polyimide nanocomposites for high-temperature capacitive energy storage, *Adv. Energy Mater.*, 2020, **10**(16), 1903881.
- 74 P. Hu, W. Sun, M. Fan, J. Qian, J. Jiang, Z. Dan, Y. Lin, C.-W. Nan, M. Li and Y. Shen, Large energy density at high-temperature and excellent thermal stability in polyimide nanocomposite contained with small loading of BaTiO<sub>3</sub> nanofibers, *Appl. Surf. Sci.*, 2018, **458**, 743.
- 75 X. Li, L. Weng, H. Wang and X. Wang, Nanoarchitectonics of BN/AgNWs/epoxy composites with high thermal conductivity and electrical insulation, *Polymers*, 2021, **13**(24), 4417.
- 76 B. Peng, P. Wang, H. Luo, G. He, H. Xie, Y. Liu, S. Chen, X. Li, Y. Wan and R. Guo, Outstanding high-temperature capacitive performance in all-organic dielectrics enabled by synergistic optimization of molecular traps and aggregation structures, *Mater. Horiz.*, 2025, **12**(4), 1223.
- 77 Y. Shang, Y. Feng, Z. Meng, C. Zhang, T. Zhang and Q. Chi, Achieving synergistic improvement in dielectric and energy storage properties at high-temperature of all-organic composites *via* physical electrostatic effect, *Mater. Horiz.*, 2024, **11**(6), 1528.
- 78 Q. Wang, T. Wang, H. Chi, D. Zhao, L. Yu, Z. Jiang and Y. Zhang, Scalable all-organic polymer dielectrics for high-temperature film capacitors with construction of deep-trap level and cross-linking network, *Chem. Eng. J.*, 2025, **506**, 160204.
- 79 D. Xu, W. Xu, T. Seery, H. Zhang, C. Zhou, J. Pang, Y. Zhang and Z. Jiang, Rational design of soluble polyaramid for high-efficiency energy storage dielectric materials at elevated temperatures, *Macromol. Mater. Eng.*, 2020, **305**(3), 1900820.
- 80 Y. Zhang, Z. Liu, L. Zhu, J. Liu, Y. Zhang and Z. Jiang, Enhanced discharged efficiency and high energy density at elevated temperature in polymer dielectric *via* manipulating relaxation behavior, *CCS Chem.*, 2020, **2**(5), 1169.